

Automatic Assessment of Scintmammographic Images Using a Novelty Filter

Marly Costa, MSc, University of Amazonas/FUCAPI - Amazonas, and Unicamp - Sao Paulo
Lincoln Moura, PhD, InCor, São Paulo Heart Institute - São Paulo University Medical School Hospital

ABSTRACT

^{99m}Tc-sestamibi scintmammograms provide a powerful non-invasive means for detecting breast cancer at early stages. This paper describes an automatic method for detecting breast tumors in such mammograms. The proposed method not only detects tumors but also classifies non-tumor images as "normal" or "diffuse increased uptake" mammograms.

The detection method makes use of Kohonen's "novelty filter". In this technique an orthogonal vector basis is created from a normal set of images. Test images presented to the detection method are described as a linear combination of the images in the vector basis. Assuming that the image basis is representative of normal patterns, then it can be expected that there should be no major differences between a normal test image and its corresponding linear combination image. However, if the test image presents an abnormal pattern, then it is expected that the "abnormalities" will show as the difference between the original test image and the image built from the vector basis. In other words, the existing abnormality cannot be explained by the set of normal images and comes up as a "novelty."

An important part of the proposed method are the steps taken for standardizing images before they can be used as part of the vector basis. Standardization is the keystone to the success of the proposed method, as the novelty filter is very sensitive to changes in shape and alignment.

INTRODUCTION

Screening for breast cancer diagnosis is an important issue as successful treatment depends on early detection. Although X-ray mammography is currently recognized as the most effective way of detecting non-palpable breast tumors^{1,2}, it has been shown that nuclear medicine images of the breast (scintmammograms) using Technetium-99m-sestamibi offer a simple non-invasive method that presents improved sensitivity and specificity for the detection of breast cancer.³

^{99m}Tc-sestamibi has been widely used for detecting myocardial ischemia and infarction.^{4,5} More recently, it has also been used for imaging several types of tumors, such as bone and thyroid tumors.^{6,7,8} Diggles and co-workers³ reported a sensitivity of 96% and a specificity of 85% when using that radiopharmaceutical for detecting breast cancer by a human expert.

One of the main problems in medical imaging is that of quantification by visual inspection. Medical examinations that comprise visual assessment of images, or even the manual definition of structure boundaries for later quantification, are likely to be strongly affected by human interaction. The potential for an oversight or "miss" by the clinician is always present.

Automatic methods, on the other hand, are not operator-dependent and are thus repeatable. Errors made by automatic methods tend to be systematic. Once validated, these methods can be extensively used, freeing the operator, reducing overall time and increasing reliability.

InCor, São Paulo Heart Institute, performs more than 1,500 heart scans per month in its Nuclear Medicine Department. The Department is currently involved in a program for the detection of breast cancer using ^{99m}Tc-sestamibi scintmammograms.

Several methods can be used for detecting tumors automatically in medical images. Of particular interest to us was the "novelty filter" technique, proposed by Kohonen⁹, as it presents important attributes regarding robustness and an ability to learn from examples.

METHODS

The Novelty Filter Concept

Let s be a set of vectors $\{v_1, v_2, v_3, \dots, v_m\} \in \mathbf{R}^n$ that spans a sub-space $L \in \mathbf{R}^n$. Any given vector $x \in \mathbf{R}^n$ can be uniquely decomposed into two vectors, \hat{x} and \tilde{x} , that are the projection \hat{x} of x onto sub-space L , and the projection \tilde{x} of x onto sub-space L^\perp , which is the sub-space that is orthogonal to L . From the Projection Theorem⁹ it comes that \tilde{x} has minimal norm. Vector \tilde{x} can be seen as the portion of x that cannot be explained

by a linear combination of the m vectors of s , and is called a *novelty*.

Decomposing x into sub-spaces L and L^\perp involves computing the projection matrix P that satisfies $\hat{x} = Px$ and $\tilde{x} = (I - P)x$. Matrix P can be computed as $P = (I - XX^+)$, where X is the matrix formed by column-vectors v_k , X^+ is the pseudo-inverse matrix of X and I is the identity matrix.

Assuming that the v_k vectors are linearly independent, matrix X^+ can be computed as $X^+ = (X^T X)^{-1} X^T$, where X^T is the transposed matrix of X .¹⁰

When dealing with images, solving those equations can be very computer-expensive, as the dimension of square matrix P will be the number of pixels in a single image (16,384 in the case of scintmammograms such as those under study in this paper).

One way to circumvent that problem is to use the well established Gram-Schmidt method¹¹ for computing \tilde{x} . This process consists of creating a new set of basis vectors that are mutually orthogonal. This is achieved by making:

$$h_1 = v_1 \quad (1)$$

and

$$h_k = v_k - \sum_{j=1}^{k-1} \langle v_k, h_j \rangle \cdot h_j / \|h_j\|^2, \text{ for } k=2,3, \dots, m. \quad (2)$$

The novelty \tilde{x} can then be computed by simply extending equation 2 one step further, so that $\tilde{x} = h_{m+1}$.

Image Acquisition

Bilateral scintmammography was performed on 33 female patients using a Siemens Gamma Camera. Each patient received 740 Mbq of ^{99m}Tc-sestamibi injected in the arm intravenously. Patients were positioned in the prone position. Images were acquired 60 minutes post-injection, at a spatial resolution of 64 x 64 pixels and 8-bit depth resolution. For every breast, three images were acquired: an 8-minute lateral image, an 8-minute 30° posterior oblique image and a 10-minute anterior chest image.

The method described in this paper makes use only of lateral images, representing 33 pairs of images, or 66 images. Of these, 10 images could not be used either because they were much too noisy, or they presented undesirable features such as a breast that underwent mastectomy or a non-breast tumor. Visual inspection by an experienced nuclear medicine clinician showed that 21 out of 66 images corresponded to normal breasts, of which, 16 were used for creating a normal breast image basis.

All scintmammograms were treated as right-breast images. Left-breast images were mirrored so that the breast position became similar to that of a right-breast image.

Pre-processing

Images were interpolated to increase their resolution to 128 x 128. Although interpolation does not increase the amount of information in the image, it reduces relative pixel size, so that there are more pixels within any given region. Image interpolation was performed directly by the imaging equipment.

Intensity normalization was performed on the interpolated images, to ensure that all images had similar energies. After intensity normalization, all images had the lowest and the highest pixel values set to 0 and 255 respectively.

One of the main problems that arise when using the novelty filter is that images in the image basis and those to be tested must be very well aligned. Structures and organs must occupy exactly the same position throughout the series of basis and test images otherwise the novelty filter either loses sensitivity or becomes too inaccurate.¹²

In order to make all breasts fit the same template, they were automatically segmented by fitting a triangle to them, using a method that is described in the next section. Once defined, the triangles were geometrically modified to match each other completely, as described ahead.

Automatic Breast Segmentation

The first step for automatic segmentation of the breast is breast contour detection. This is carried out by scanning all image lines, from right to left in search of a sequence of pixel values that are greater than a given threshold. This procedure results in edge images. Figure 1a shows a detected edge image superimposed onto its corresponding

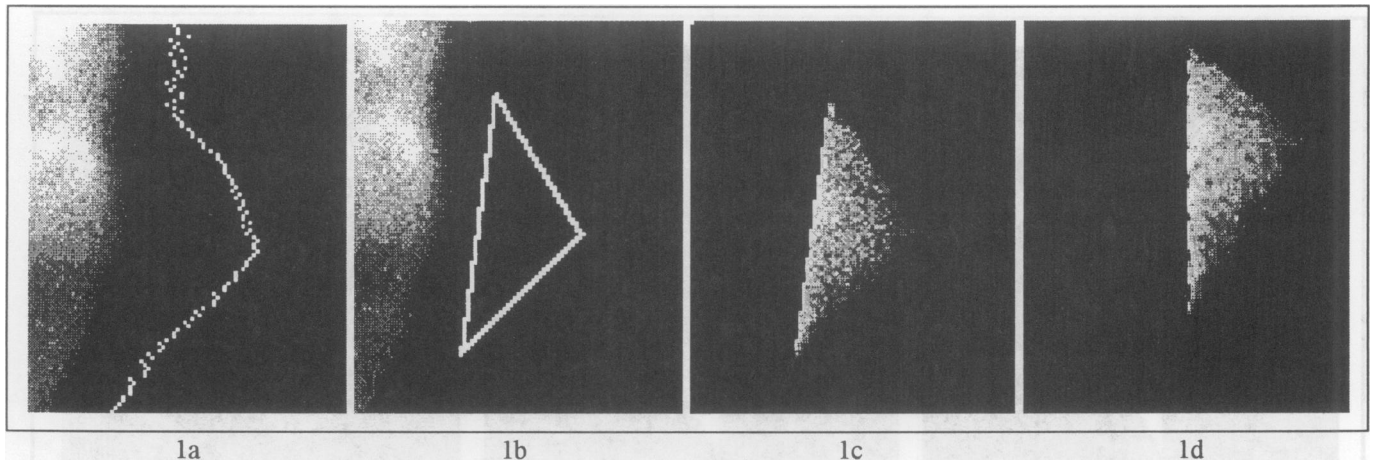


Figure 1. In (1a) the breast edge image is superimposed onto the original image; In (1b) the detected triangle is shown, superimposed onto the breast image; Figure (1c) shows the region where novelties will be searched for, after histogram stretch, and Figure (1d) shows the same region after being standardized to match the region defined by the reference breast.

original image. The next steps consist of detecting the vertices of the triangle that defines the breast. The rightmost edge pixel defines the breast's nipple. The 20 uppermost lines are scanned and the edge pixel with the greatest x -coordinate (rightmost pixel) determines a vertical line. The breast edge is scanned upward from the nipple until an edge pixel falls to the left of the vertical line. That pixel defines the second triangle vertex. A similar procedure is carried out on the 20 lowermost lines for the detection of the third triangle vertex.

The region within the triangle is the region that must be looked for novelties and is extracted from the image, resulting in a segmented image similar to that shown in figure 1c. Histogram stretch was performed on segmented images in order to achieve intensity normalization. That operation consisted of stretching 99% of the unprocessed image's histogram to fit the whole depth range as proposed by Moura.¹³

Standardization

Standardization is the most important single step for the success of the novelty filter. As the detected triangles present different shapes and areas, the regions they define should be geometrically modified so that they completely match.

Standardization consists basically of mapping the pixels within one image's triangle to a reference breast triangle. The mapping involves rotation, translation, scaling and interpolation of image regions. Interpolation was always performed using a bi-linear algorithm. Figure 1d shows

the breast of image 1a after being modified to fit the region defined by the reference breast.

Normal Breast Vector-Basis

A set of 16 normal scintmammograms was chosen at random from the data set, aiming at the creation of an image basis for normal breasts.

All 16 breast images were pre-processed and segmented using the procedures previously described.

The triangle whose surface area was closest to the average breast surface area was chosen as the reference breast contour to which all other breasts would be matched. The 15 remaining normal breast triangles were then standardized to match the reference breast, thus leading to a set of 16 standardized normal breast images.

Orthogonalization

An orthogonal image basis was obtained from the standardized image basis by using the Gram-Schmidt method previously described. That method assumes basis images are linearly independent. In order to certify that, the dot product between any two images in the orthogonal basis was monitored and was ensured to be less than a certain threshold.

Image Analysis

Once the orthogonal standardized image basis was created it was possible to test new images. Testing new

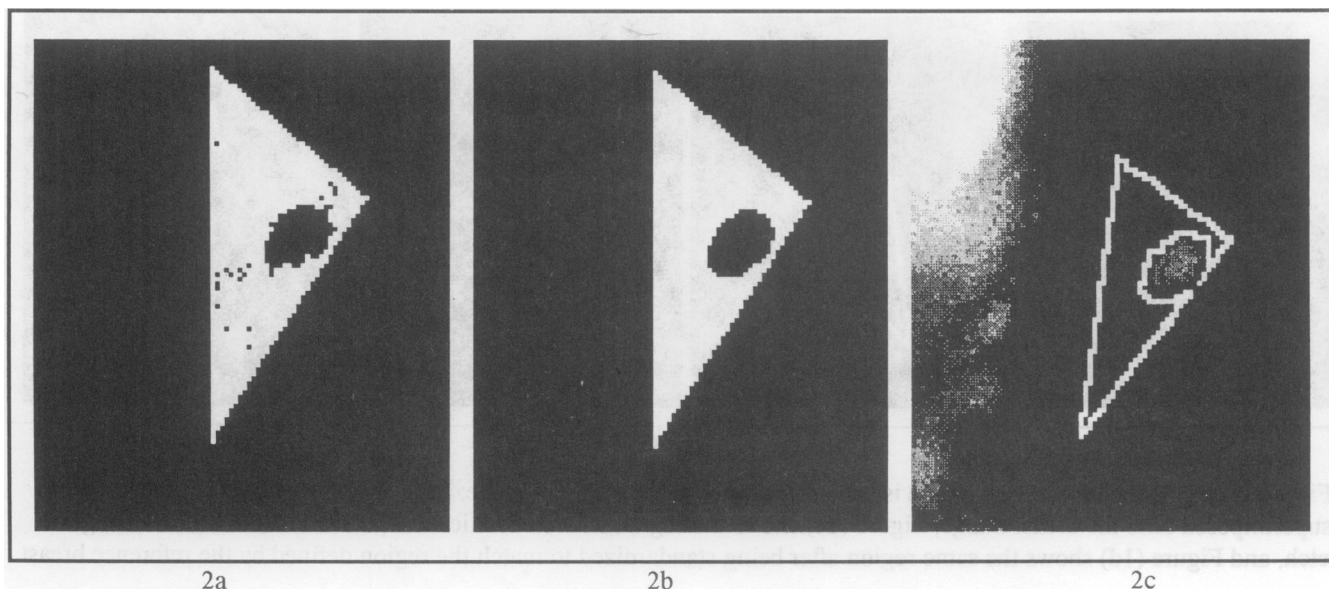


Figure 2. Figure 2a shows the novelty found for a focal uptake breast; In (2b) the novelty is shown after morphological filtering, clearly showing a tumor; Figure (2c) shows the novelty mapped back onto the original image, thus allowing for the assessment of exact tumor location and geometry.

images always involves undergoing all those steps that result in a standardized image and then describing it as a linear combination of all images in the basis using equation 2, as discussed in a previous section of this paper.

Images that represent normal breasts should yield no novelty, whereas images representing diseased breasts should contain patterns that cannot be explained by a linear combination of normal breast images.

In fact it was noticed that image regions that corresponded to focal uptake led to high positive novelty values. Figure 2a shows a novelty image of a focal uptake (tumor) and figure 2b shows the same image after some morphological filtering for noise reduction and better tumor definition. Once a tumor is detected in a standardized image, it is mapped back onto the original image -- in a process that is the inverse of standardization -- so that the tumor's real position and geometry can be seen (figure 2c).

One of the functions of the morphological filter is to detect whether the set of pixels that comprise the novelty is highly connected or not. After filtering, connected pixel regions greater than 23 pixels are considered to be tumors. Regions with less than that number of pixels are considered to be part of diffuse uptake regions. If no region contains more than 23 connected pixels the image corresponds to diffuse uptake.

RESULTS

Forty scintmammograms were analyzed by both an experienced nuclear medicine physician and the proposed novelty filter. No mammograms were available for those patients. The test scintmammograms were classified by the clinician as 5 normal breasts, 15 breasts with diffuse increased uptake and 20 breasts with focal uptake (tumor). The images under study comprised lesions of varied degrees of severity and subtlety. All tumors were malignant.

The results of the automatic analysis are summarized in Table 1, and show that the method presents good sensitivity for detecting both tumors and diffuse uptake. It also presents a good positive predictive value for malignant tumors.

Table 1

Clinician's Diagnosis	Automatic Detection by the Novelty Filter			Totals
	Normal	Diffuse Uptake	Focal Uptake	
Normal	5	0	0	5
Diffuse Uptake	2	12	1	15
Focal Uptake	1	1	18	20

The proposed method was able to correctly detect 18 out of 20 malignant tumors (focal uptake), 5 out of 5 normal breast images and 12 out of 15 diffuse uptake images.

Values in Table 1 lead to a sensitivity of 90% and a specificity of 95%, for detecting tumors, a sensitivity of 80% and a specificity of 96%, for detecting diffuse uptake breasts and a sensitivity of 100% and a specificity of 91.4% for detecting normal subjects.

The positive predictive value for detecting tumors is 94.7%, for diffuse uptake it is 92.3% and for normal subjects it is 62.5%.

CONCLUSIONS

The authors firmly believe that, although good, results can be improved by improving the normal breast image-basis and the image data set. The currently in use data set consisted of images that were analyzed only by visual inspection. The total number of normal breast images that could be used by the system was only 21 (16 used for creating the basis and 5 for testing). Our major concern, at the moment, is to increase the image data set to include some 100 normal breasts and have a histological test to confirm the clinician's evaluation.

The proposed method has been implemented on a 486DX66 MHz microcomputer. The time for image analysis - including pre-processing and standardization - is around 1 minute, thus allowing the method to be a valuable complementary tool for the screening of scintimammograms.

The choice of a novelty filter for performing the automatic assessment of scintimammograms seems to have been worth it, as the resulting system is robust and versatile.

Future work should focus on using the other image projections that are routinely acquired to create a different image basis and different criteria for standardization. Also, if tumors are to be contoured automatically, fitting a triangle to the breast contour may be unsuitable, as it can miss part of a tumor. We are working on a model that fits two parabolas to the detected breast contour, thus involving the entire breast.

ACKNOWLEDGMENTS

The authors are indebted to Dr Cláudio Meneghetti, MD, Head of InCor's Nuclear Medicine Department, for giving important general guidelines, and to Mr Marco Antonio Oliveira for providing them with the image data set. This work was partly supported by FAPESP, São Paulo State Research Agency (grant 92/0577-8).

References

1. Kopans DB. The positive predictive value of mammography. *AJR* 1992;158:521-5262.
2. Martin J, Moskowitz M, Milbrath JR, Breast cancer missed by mammography, *AJR* 1979; 132:737-739.
3. Diggles L, Mena I, Khalkhali I. Technical aspects of prone dependent-breast scintimammography. *J Nucl Med Tech.* 1994; 22: 165-170.
4. Baillet GY, Mena I, Kuperus JH, Robertson JM, French WJ. Simultaneous Tc-99m-MIBI angiography and myocardial perfusion imaging. *J Nucl Med.* 1989, 30:38-44.
5. Narahara K A, Villanueva-Meyer J, Thompson CJ, Brizendine M, Mena I. Comparison of thallium-201 and technetium-99m-hexakis 2-methoxy-isobutyl isonitile single-photon emission computed tomography for estimating the extent of myocardial ischemia and infarction in coronary artery disease. *Am J Cardiol.* 1990; 66:1438-1444.
6. Balon HR, Fink-Bennett D, Stoffer SS. Technetium-99m-sestamibi uptake by recurrent Hurthle cell carcinoma of thyroid. *J Nucl Med.* 1992; 33:1393-1395.
7. Coakley AJ, Kettle AG, Wells CP, et al. Thechnetium-99m-sestamibi: a new agent for parathyroid imaging. *Nucl Med Commun.* 1989; 10:791-794.
8. Caner B, Kitapçl M, Mustafa U, et al. Technetium-99m-sestamibi uptake in benign and malignant bone lesions: a comparative study with technetium-99m-MDP. *J Nucl Med* 1992;33:319-324.
9. Kohonen T. Self-organization and associative memory. New York: Springer-Verlag, Inc.1989.
10. Albert A. Regression and the Moore-Penrose pseudoinverse. New York: Academic Press, Inc. 1972.
11. Landesman EM, Hestenes MR. Linear algebra for mathematics, science and engineering. New Jersey: Prentice-Hall International, Inc.1992.
12. Raf U and Newman FD. Automated lesion detection and lesion quantitation in MR images using autoassociative memory. *Med Phys.* 1992, 19:71-77.
13. Moura L and Kitney R. Automatic Reconstruction of 3D Coronary Artery Segments. *Automedica*, Volume 15, Number 2 (1992), pp 97-121.